Sulphate, dissolved organic carbon, nutrients and terminal metabolic products in deep pore waters of an intertidal flat

Melanie Beck · Olaf Dellwig · Jan M. Holstein ·
Maik Grunwald · Gerd Liebezeit ·
Bernhard Schnetger · Hans-Jürgen Brumsack

Abstract This study addresses deep pore water chemistry in a permeable intertidal sand flat at the NW German coast. Sulphate, dissolved organic carbon (DOC), nutrients, and several terminal metabolic products were studied down to 5 m sediment depth. By extending the depth domain to several meters, insights into the functioning of deep sandy tidal flats were gained. Despite the dynamic sedimentological conditions in the study area, the general depth profiles obtained in the relatively young intertidal flat sediments of some metres depth are comparable to those determined in deep marine surface sediments. Besides diffusion and lithology which control pore water profiles in most marine surface sediments, biogeochemical processes are influenced by advection in the studied permeable intertidal flat sediments. This is supported by the model setup in which advection has to be implemented to reproduce pore water profiles. Water exchange at the sediment surface and in deeper sediment layers converts these permeable intertidal sediments into a "bio-reactor" where organic matter is recycled, and nutrients and DOC are released. At tidal flat margins, a hydraulic gradient is generated, which leads to water flow towards the creekbank. Deep nutrient-rich pore waters escaping at tidal flat margins during low tide presumably form a source of nutrients for the overlying water column in the study area. Significant correlations between the inorganic products of terminal metabolism (NH_4^+ and PO_4^{3-}) and sulphate depletion suggest sulphate reduction to be the dominant pathway of anaerobic carbon remineralisation. Pore water concentrations of sulphate, ammonium, and phosphate were used to elucidate the composition of organic matter degraded in the sediment. Calculated C:N and C:P ratios were supported by model results.

M. Beck (✉) · O. Dellwig · M. Grunwald ·
B. Schnetger · H.-J. Brumsack
Research Group Microbiogeochemistry, Institute for
Chemistry and Biology of the Marine Environment
(ICBM), Carl von Ossietzky University, PO Box 2503,
26111 Oldenburg, Germany
e-mail: m.beck@icbm.de

O. Dellwig
Leibniz Institute for Baltic Sea Research IOW,
Seestraße 15, 18119 Rostock, Germany

J. M. Holstein
Research Group Mathematical Modelling, Institute for
Chemistry and Biology of the Marine Environment
(ICBM), Carl von Ossietzky University, PO Box 2503,
26111 Oldenburg, Germany

G. Liebezeit
ICBM-Terramare, Schleusenstraße 1,
26382 Wilhelmshaven, Germany

Introduction

It has been demonstrated that sand flats with low organic carbon contents have rates of organic matter

remineralisation comparable to those of organic rich muds (Rusch et al. 2006). The permeability of sand facilitates advective pore water transport in contrast to diffusion-controlled muddy sediments. Rapid exchange between pore water and the overlying water column has been identified as the most important process responsible for enhanced remineralisation rates and carbon cycling in sands. In both sandy and muddy sediments water exchange in the upper sediment layers is facilitated by bioturbation. In sand flats, pore water flow in the upper decimetres of permeable sandy sediments is further enhanced due to pressure gradients. These are generated during inundation by the interaction of bottom currents with sediment topography like ripples (Huettel et al. 1996; Huettel and Rusch 2000; Precht and Huettel 2004). The induced pore water flow at the sediment surface is an effective mechanism for rapid exchange of oxygen (Ziebis et al. 1996; Precht et al. 2004; Rusch et al. 2006), dissolved and particulate organic matter (Huettel et al. 1996; Huettel and Rusch 2000; Rusch and Huettel 2000; Rusch et al. 2001), and nutrients (Caetano et al. 1997; Huettel et al. 1998) in permeable sediments. Consequently, advective pore water exchange at the sediment surface leads to fast recycling of organic matter and the removal of metabolic products within a time range of hours and/or days.

Processes of organic matter mineralisation were described in numerous studies concerning deep marine and coastal sediments. The dominant organic matter mineralisation pathways vary depending on the availability of the electron acceptors oxygen, nitrate, manganese oxides, iron oxides or sulphate. Nitrate reduction is of minor importance (<10%) for C oxidation in coastal sediments (Sørensen et al. 1979; Canfield et al. 1993a). The contributions of manganese and iron reduction to C oxidation are less frequently determined. In many sediments their contributions are small, but gain importance in Mn- or Fe-rich sediments (Canfield et al. 1993b; Thamdrup and Canfield 1996). Determinations of sulphate reduction rates in sediments are numerous and have shown that this pathway accounts for 10–90% of the C oxidation in coastal sediments (Jørgensen 1982; Thamdrup and Canfield 1996; Gribsholt and Kristensen 2003).

In tidal flat sediments, nutrients and dissolved organic carbon (DOC) were examined by several authors (Howes and Goehringer 1994; Böttcher et al.

1998; Böttcher et al. 2000; Jahnke et al. 2003; de Beer et al. 2005; Kuwae et al. 2003; Billerbeck et al. 2006b; Magni and Montani 2006; Murray et al. 2006; Weston et al. 2006). However, there are few studies which focused on these species in sediment depths exceeding 1 m. Charette and Sholkovitz (2006) determined nutrients and DOC down to about 8 m depth in a subterranean estuary of Waquoit Bay, USA, but focused on trace elements. Concerning tidal flat sediments, there is thus little knowledge about biogeochemical processes occurring in pore waters deeper than the sediment surface. It is not known whether in relatively young tidal flat sediments of some metres depth, similar biogeochemical processes occur than in surface sediments of deep marine environments.

In this study, sulphate, DOC, nutrients, and several terminal metabolic products were for the first time determined in pore waters down to 5 m depth in an intertidal flat from the NW German coast. Pore water analyses were complemented by a geochemical characterisation of the sedimentary column required to understand pore water profiles. In contrast to previous studies which focussed on surface sediments, we try to decipher biogeochemical processes and organic matter remineralisation pathways in deep intertidal flat sediments. Biogeochemical processes deduced from pore water results were verified by a model setup.

Materials and methods

Study area

The Wadden Sea, located in the Southern North Sea, forms one of the largest tidal flat areas of the world extending for almost 500 km between Den Helder (Netherlands) and Skallingen (Denmark). In Northwest Germany, the tidal flat area is located between the coastline and a chain of barrier islands, which are separated by tidal inlets. These inlets connect the tidal flat areas with the open North Sea. The tidal flat area itself is divided by a large main channels and smaller secondary channels. Sampling was carried out on the Eastern margin of the intertidal sand flat Janssand, located in the backbarrier area of the Island of Spiekeroog (53° 44,183′ N; 007° 41,904′ E; Fig. 1). The study area is characterised by semidiurnal tides and a tidal range of 2.6 m (Flemming

and Davis [1994]). During high tide, the Janssand tidal flat is covered by 1–2 m of water. It becomes exposed to the atmosphere for approximately 6 h, depending on tidal range and wind direction. The Janssand tidal flat surface is almost horizontal, except for the margin where the sediment surface slopes towards the main tidal channel. During low tide the distance between the sampling location and the water line is

Fig. 1 (**a**) Study site in an intertidal sand flat (Janssand) in the backbarrier area of Spiekeroog Island, Wadden Sea, Germany. (**b**) Tidal flat topography

approximately 70 m and the difference in altitude amounts to about 1.5 m.

Sample collection

Pore water

Pore water sampling was carried out using in situ samplers described in more detail in Beck et al. ([2007]). Each sampler is composed of a polyethylene (PE) pipe with sampling ports at different depths down to 5 m. Teflon tubings link the sampling orifice to sampling devices located at the sediment surface. Each in situ pore water sampling system consists of two samplers. The short sampler (1 m length) has 11 sampling ports at 0.05, 0.07, 0.10, 0.15, 0.20, 0.25, 0.30, 0.40, 0.50, 0.75, and 1.0 m sediment depth. The long sampler (5 m length) has 10 sampling ports located at 1.0, 1.25, 1.5, 2.0, 2.5, 3.0, 3.5, 4.0, 4.5, and 5.0 m sediment depth. At the top of the sampler PE syringes can be connected to the sampling system to extract pore water from the sediment. Depending on sampling depth and diameter of the teflon tubes, different volumes of pore water were discarded before taking samples for analyses. All samples were pre-filtered through nylon gauzes of 100 and 50 μm pore size located in front of the sampling orifices and immediately filtered through 1.2 μm GF/C filters after extraction.

Pore water samples were taken on April 25th, 2006 except for methane samples which were retrieved on March 22nd, 2006. To elucidate organic matter composition, data from May 2005 to June 2006 are further used. Samples were analysed for nutrients (NH_4^+, PO_4^{3-}, H_4SiO_4, NO_3^-), sulphate (SO_4^{2-}), sulphide (H_2S), methane (CH_4), dissolved organic carbon (DOC), total alkalinity (TA) and chloride (Cl^-). Furthermore, the pH value was measured on site using an aliquot of the sample (pH/Cond 340i, WTW, Weilheim, Germany). Samples for the analysis of nutrients, TA, SO_4^{2-}, and Cl^- were stored in PE vials. Samples for DOC analyses were acidified by adding 1 ml HCl (6 M) to 40 ml sample and stored in glass bottles. All PE vials were pre-rinsed with ultrapure water prior to use, while all glass bottles were acid washed and rinsed with ultrapure water. All samples were stored at 4–6 C until analysis. The determination of nutrients was conducted the day after sampling.

For the determination of H_2S, a certain volume of sample, depending on the expected H_2S concentration,
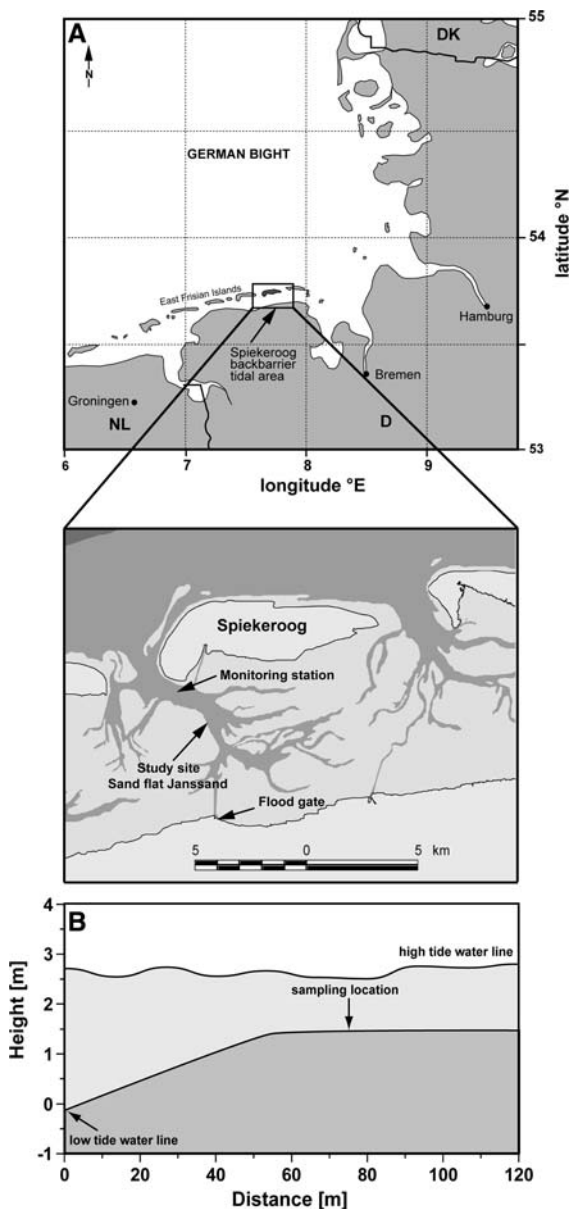
was added to 5 ml of a 10 mM Cd-acetate solution immediately after sampling. The addition of sample was stopped when yellow fluffs of CdS started to precipitate. Samples for CH_4 analysis were filled from the syringe into headspace vials with rubber septa and aluminium crimp seals, and immediately frozen in the field. Degassing of the sample has to be taken into account because of pore water extraction by vacuum. However, analyses of CH_4 in sediment cores taken close to the pore water sampling site showed similar results suggesting that degassing is rather limited.

Sediment core

Within a distance of some metres to the pore water samplers a sediment core was collected in April 2005. An aluminium tube with a diameter of 8 cm was driven into the sediment by a vibration corer to a depth almost equivalent to the length of the sampler. Sampling of the sediment core was carried out depending on changes in lithology.

Pore water analysis

Nutrients

Nutrient concentrations (NH_4^+, PO_4^{3-}, H_4SiO_4, NO_3^-) were determined photometrically by methods described in Grasshoff et al. (1999) using a spectrophotometer (Spekol 1100, Analytik Jena). Samples containing high concentrations of sulphide were diluted to reduce the effect of sulphide on the formation of coloured complexes, especially for the determination of PO_4^{3-} and H_4SiO_4. Total alkalinity was determined by a spectroscopic method proposed by Sarazin et al. (1999). Solutions containing known concentrations of the analytes were used to check precision and accuracy of the measurements. Precision/accuracy were 5.6%/−2.5% for alkalinity (at 2.5 mM), 5.1%/−3.0% for NH_4^+ (at 1 mM), 4.8%/1.2% for PO_4^{3-} (21 μM), and 4.1%/2.7% for H_4SiO_4 (at 142 μM).

Sulphate

SO_4^{2-} was analysed by ion chromatography (Dionex DX 300) in a 250-fold dilution, with standard Atlantic Seawater (Salinity 35.0 (± 0.2%); OSIL, UK) used to control the precision (3.0%) and accuracy (−5.3%) of the measurements.

Sulphide

For the analysis of H_2S the solution containing the yellow CdS precipitate was filtered through a 0.2 μm syringe filter. The filter was washed with 5 ml 1% (v/v) formic acid and 10 ml ultrapure water to dissolve Cd carbonates also retained on the filter and to remove any excess Cd that did not react with H_2S. The yellow precipitate on the filter was dissolved by adding 10% HCl (v/v), and the filtrate was made up to a constant volume. Cd was analysed by FAAS (Perkin Elmer AAS 4100) and the H_2S concentration in the samples was calculated based on the Cd concentrations measured as well as CdS stoichiometry.

Dissolved organic carbon

DOC was analysed by high temperature catalytic oxidation using a multi N/C 3000 analyser (Analytik Jena, Jena, Germany). Prior to the determination of DOC, the acidified samples were purged by synthetic air to remove any dissolved inorganic carbon. Potassium hydrogen phthalate solutions were used for external calibration and to control precision and accuracy of the measurements. Precision was better than 2.4% and accuracy better than 1.9%.

Chloride

Cl^- was determined by micro titration using a 0.1 mM $AgNO_3$ solution to titrate a solution composed of 100 μl sample, 5 ml ultrapure water and 100 μl of a K-chromate/-dichromate solution (4.2 g and 0.7 g, respectively, dissolved in 100 ml ultrapure water). Standard sea water of salinity 30.005 (OSIL, UK) was used to control the precision (0.41%) and accuracy (−0.11%) of the measurements.

Methane

For measuring methane concentrations, gas from the headspace of the bottles was injected into a CX-3400 gas chromatograph (Varian, Darmstadt, Germany) equipped with a capillary column (plot-fused silica column no. 7517, 25 m by 0.53 mm, Al_2O_3/KCl coated; Chromopack, Middelburg, The Netherlands) and measured by a flame ionisation detector. Accuracy (2.9%) and precision (13.9%) were controlled by a 100 ppmv standard of methane.

Sediment analysis

XRF

Sediment samples were freeze dried and homogenised in an agate mill. All samples were analysed for the elements Si, Al, Ti, and Zr by XRF using a Philips PW 2400 X-ray spectrometer. 600 mg of sample were mixed with 3600 mg of a mixture of dilithiumtetraborate/lithiummetaborate (50% $Li_2B_4O_7$/50% $LiBO_2$), pre-oxidised at 500° C with NH_4NO_3 (p.a.), and fused to glass beads. Analytical precision and accuracy were better than 5% for all elements.

Bulk parameters

Total carbon (TC) and total sulphur (TS) were determined using an CS 500 IR analyser (Eltra, Neuss, Germany), while total inorganic carbon (TIC) was analysed coulometrically by a CM 5012 CO_2 coulometer coupled to a CM 5130 acidification module (UIC, Joliet, USA). Total organic carbon (TOC) was calculated as the difference between TC and TIC. Total nitrogen (TN) was analysed by an Carlo Erba Element Analyser EA 1108. Precision and accuracy of TC and TIC analyses were better than 3% and 1%, respectively.

Calculation of sulphate depletion, C:N, and C:P ratios

Sulphate depletion

The SO_4^{2-} depletion in pore waters was calculated using the concentrations determined for the specific sediment depths (Sholkovitz 1973; Weston et al. 2006). The depletion in SO_4^{2-} reflects the net amount of SO_4^{2-} consumption, presumably via bacterial SO_4^{2-} reduction, and was calculated according to

$$\left(SO_4^{2-}\right)_{Dep} = \left[\left(Cl_{PW}^-\right) \cdot \left(R_{SW}\right)^{-1}\right] - \left(SO_4^{2-}\right)_{PW} \quad (1)$$

where $(SO_4^{2-})_{Dep}$ is the SO_4^{2-} depletion, $(Cl^-)_{PW}$ and $(SO_4^{2-})_{PW}$ are the pore water concentrations of Cl^- and SO_4^{2-}, and R_{SW} is the molar ratio of Cl^- to SO_4^{2-} in surface sea water ($R_{SW} = 19.33$). A hypothetical SO_4^{2-} concentration at a specific depth interval is calculated by using Cl^- data. Slight changes in salinity due to rain or fresh water input

are thus compensated. The difference between the hypothetical and the measured SO_4^{2-} concentration forms an estimate for the metabolic amount of SO_4^{2-} reduction.

Ratios

Carbon to nitrogen (C:N) and carbon to phosphorus (C:P) stoichiometry of the organic matter degraded was estimated by regression analysis of $(SO_4^{2-})_{Dep}$ against NH_4^+ and PO_4^{3-} and multiplying the ratios of $(SO_4^{2-})_{Dep}$ to NH_4^+ and PO_4^{3-} by a factor of 2. This estimation is based on the assumption that the ratio of C to SO_4^{2-} is 2:1 if the oxidation of organic matter is coupled to sulphate reduction according to the equation

$$(CH_2O)_{106}(NH_3)_{16}H_3PO_4 + 53SO_4^{2-} + 14H^+$$
$$\rightarrow 53H_2S + 16NH_4^+ + H_2PO_4^- + 106HCO_3^- \quad (2)$$
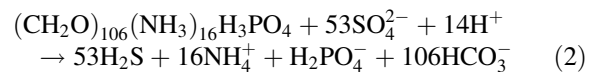
where organic matter composition follows the Redfield relationship. Using the Redfield formula represents an approximation. The formula is based on living marine phytoplankton and is thus uncertain for buried organic matter (Sholkovitz 1973). A further approximation is the estimation of the $C:SO_4^{2-}$ ratio in the pore water samples by a regression analysis of $(SO_4^{2-})_{Dep}$ against TA. Dissolved inorganic carbon (DIC) should be used for the determination of the $C:SO_4^{2-}$ ratio. Calculating DIC concentrations by using a program developed for CO_2 system calculations (Lewis and Wallace, 1998) revealed that TA equals DIC except at 5 m depth where a slight pH decline is observed (Fig. 5). The use of TA instead of DIC has thus very minor implications for the results. TA concentrations are used for regression analyses because of missing pH values for some sampling campaigns. All ratios were further corrected by the appropriate diffusion coefficients described by Boudreau (1997) for HCO_3^-, SO_4^{2-}, NH_4^+ and PO_4^{3-}. The C:N ratio of the organic matter being mineralised was estimated from the linear regression of TOC against TN determined in sediment samples of April 2005.
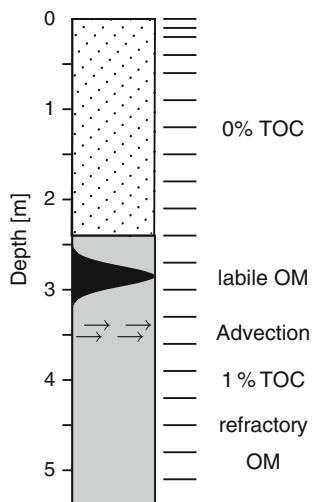
Model setup and pore water modelling

Pore water modelling was conducted to reproduce the observed pore water profiles under the assumption of advective pore water flow. The applicability of the

regression technique for sites with advective lateral exchange was further evaluated by comparing the respective C:N:P ratios with those of in situ decomposing organic matter in the model setup. For modelling the pore water profiles, the generic computer model ISM (integrated sediment model) was used (Wirtz 2003). It is a partial differential equation model describing diffusive transport and biogeochemical processes in aquatic porous media. The redox processes are conducted by functional groups of bacteria and bacterial growth is simulated. The model description is confined to the capabilities of the model that have been applied in this study. The model is implemented in C++ and solved using a 3rd order Runge Kutta integration method.

In the model setup an idealised sediment column is considered, which is free of organic matter in the upper part (0–2.5 m) and contains 1% TOC in the lower part (2.5–5 m) (Fig. 2). The model column is composed of 20 boxes with slightly higher resolution near the surface (Fig. 2). At 3.5 m depth horizontal advection is simulated. Above the advective layer is a zone rich in labile organic matter. Apart from this zone, organic matter is refractory. The shapes of the pore water profiles are controlled by organic matter degradation and subsequent nutrient release to pore waters, by diffusion and advective flow. The model

was calibrated to fit the observed pore water profiles by varying advection intensity, rate of decay, and C:N:P ratios of labile and refractory organic matter. Model fitness was evaluated after the model reached its steady-state.

Special emphasis was put on the organic matter remineralisation process (Fig. 3). According to Boudreau (1992), particulate organic carbon (POC) exists in two qualities (POC_1 is labile and POC_2 is refractory). POC hydrolysis is implemented as a first order decay process depending on ambient temperature T via the nonlinear Q_{10} temperature term after van't Hoff's rule. Upon hydrolysis, NH_4^+, PO_4^{3-}, and H_4SiO_4 are released according to the quality-class specific C:N:P:Si ratios. The carbon is distributed to the DOC pools (labile and refractory)
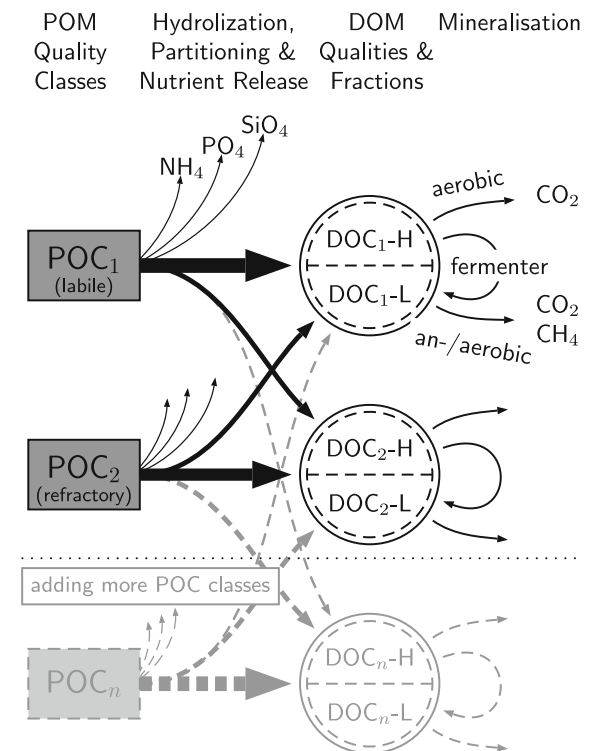
Fig. 3 Organic matter degradation scheme of the integrated sediment model. POC quality classes are converted to DOC classes according to the distribution vectors. Upon hydrolysis, nutrients are released. The distribution scheme may be extended by further POC classes (grey and dashed arrows). DOC is separated into high and low molecular weight DOC (DOC-H and DOC-L). Larger molecules (DOC-H) can only be degraded by aerobic heterotrophs or must be converted to smaller units (DOC-L) by fermenting bacteria. All heterotrophic functional groups can use DOC-L for catabolic processes

Fig. 2 Sketch of model sediment column. The upper part is free of organic matter (OM). The lower part contains 1 % total organic carbon (TOC), most of which is refractory (grey), however, there is a layer of labile OM around 2.8 m depth. Advection is indicated by arrows. The division into 20 boxes is indicated by lines

according to the distribution vectors. The effect on cross distribution is indicated in light grey dashed arrows. Each DOC quality class is split into high and low molecular weight DOC (DOC-H and DOC-L) by a global fractioning coefficient. DOC-H can be degraded by aerobic heterotrophs to CO_2 or by fermenting bacteria to DOC-L. DOC-L acts as an electron donor for all six heterotrophic functional groups of bacteria $Abac_m$ ($m = 1$–6) for catabolic processes according to the scheme of Froelich et al. (1979). The POC hydrolysis rate is proportional to the POC mass to the power of 2/3 because enzymatic processes depend on the surface of organic particles, which is simplified as sphere. POC hydrolysis is further enhanced by enzymatic activity that relates to the abundances of active bacteria $Abac_m$ and their specific yield factor on DOC. The POC hydrolysis rate of concentration C_{POC} with the quality j is

$$\dot{C}_{POC,j} = -\frac{(1-\phi)}{\phi} \cdot Q_{10}^{(T-TS)/10} \cdot C_{POC,j}^{2/3} \cdot r_j \\ \cdot \left(1 + h \cdot \sum_{m=1}^{6} y_m \cdot Abac_m\right) \tag{3}$$

were ϕ is the porosity, r_j the specific rate constant (1/d) for quality j, and h the enzymatic enhancement coefficient. Further parameters are summarised in Table 1. Due to the steady-state requirement, bacterial biomass only shows small variations resulting from the annual temperature cycle. Thus, the enzymatic enhancement term in Eq. 3 (in brackets) becomes nearly constant. In the zone of labile organic matter, approximately 30% of the POC hydrolysis rate relates to enzymatic enhancement, while in the organic matter free zone there is no enhancement.

Table 1 Parameters of the model setup

Parameter	Symbol	Value
Sediment temperature	T	Time series (Beck et al. 2008)
Standard temperature	TS	294 K
Temperature increase reaction factor	Q_{10}	2
Specific rate constant for labile organic matter	r_1	8.0×10^{-6} 1/d
Specific rate constant for refractory organic matter	r_2	1.9×10^{-6} 1/d
Porosity	ϕ	0.5

Diffusion is implemented according to Fick's second law. Diffusion coefficients are used according to Boudreau (1997). Since horizontal chemical gradients as well as horizontal flow velocities at the study site are unknown, a one dimensional column setup was chosen to limit uncertainties in model calibration. In this setup, advective flow is realised by a surrogate process. Non-local transport is a suitable substitute for advection since it connects a box directly to a pool of water which exhibits the concentrations C_0 of the species i. Instead of flow velocity, the controlling parameter is the dilution coefficient β.

$$\dot{C}_i = \beta\,(C_{0,i} - C_i). \tag{4}$$

The best fit to the field data was obtained by using a dilution coefficient of 0.005 1/d, which implies a turnover of the zone of pseudo-advection in 200 days. The model, however, is fairly insensitive to the dilution coefficient. A variation by one order of magnitude resulted in no principal change of profile shapes (not shown). The concentrations of introduced water were derived from pore waters of central parts of the tidal flat because pore water presumably flows from the central parts towards the margins of tidal flats. The concentrations applied in the model are average pore water concentrations determined at 17 different depths down to 3.5 m at a location in the central part of the tidal flat (23 mM SO_4^{2-}, 1.0 mM H_2S, 0.4 mM DOC, 0.4 mM NH_4^+, 0.5 mM PO_4^{3-} and 0.2 mM H_4SiO_4). Seasonal sea water concentrations measured in the backbarrier area of Spiekeroog are used as upper boundary conditions for the modelled column stem (unpublished data). At the lower boundary, concentrations are kept constant reflecting the quasi-linear gradients of pore water species in the lower part of the column.

Results

Sediment geochemistry

Higher amounts of coarse-grained quartz are reflected by enrichments in SiO_2, whereas higher clay contents are characterised by enrichments in Al_2O_3. At the sampling site the SiO_2 content of the sediment exceeds 80% down to 1.8 m depth, whereas below SiO_2 contents vary between 60% and 90% (Fig. 4). In
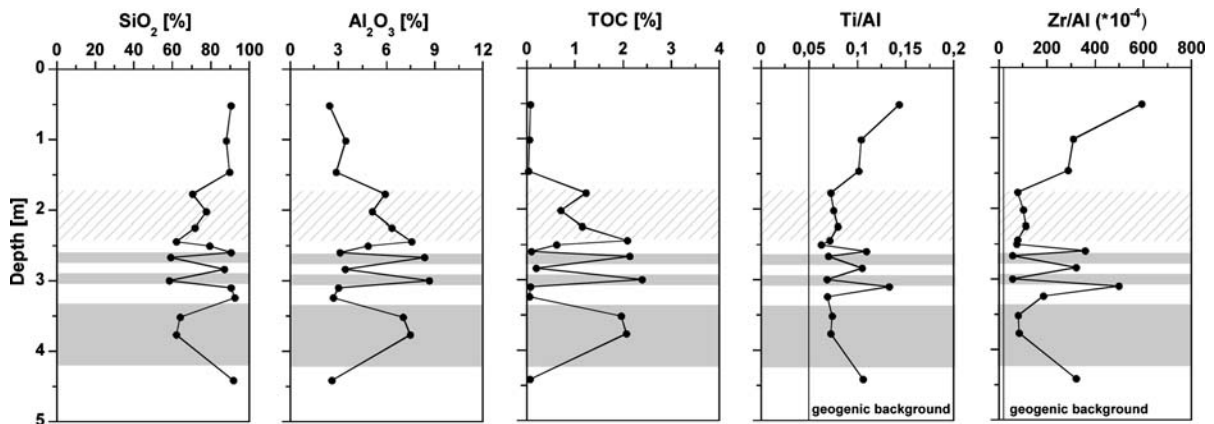
Fig. 4 Depth profiles of parameters characterising the lithology at the sampling site in an intertidal sand flat. The continuous lines in Ti/Al and Zr/Al figures indicate the geogenic background (Wedepohl 1971). The grey bars highlight the clay rich layers of the sediment profile. Depths of about 1.5 to 2.5 m are marked with a hatched area because the lithological description shows that the sediment is predominantly sandy, with very thin clay layers

depths exceeding 1.8 m, the Al_2O_3 content ranges from about 3 to 9%. The lithology is thus composed of sandy sediment intermingled by clay lenses down to 3 m depth, a clay layer at 3 m depth, a sandy layer below and clayey sediments at depths exceeding 4 m depth. Additional Al_2O_3 rich intervals shown in Fig. 4 reflect very thin clay layers or lenses. Due to lithological inhomogeneity in the sampling area, the lithology of the sediment core presumably differs slightly from the lithology at the pore water sampling site. The lithological structure of the sediment core, however, reproduces well the general sequence of sediment layers typically found in the sampling area.

The content of total organic carbon (TOC) varies between 0.04% and 2.4% with the highest values found in clay-rich layers (Fig. 4). These TOC contents are typical for sediments in the study area (Dellwig et al. 2000). TOC shows positive correlations with clay content indicating the importance of organic matter sorption onto clay particles for preservation of both marine and terrestrial organic matter (Baldock et al. 2004; Mayer 1994; Delafontaine et al. 1996).

The elements Ti and Zr are indicators of the energetic conditions prevailing during the deposition of the sediment. In Fig. 2, Ti/Al and Zr/Al ratios are displayed instead of Ti and Zr contents. Normalisation to Al eliminates dilution effects caused by quartz, carbonates, and organic matter. Any deviation from average shale composition (Wedepohl 1971) is easily recognised in element/Al ratios. High Ti/Al

and Zr/Al ratios point towards elevated heavy mineral contents (e.g. ilmenite, rutile, zircon), which are found in layers deposited under high current velocities. Clay minerals in contrast are deposited during low energy conditions. At our sampling site, the depth profiles of Ti/Al and Zr/Al show that the depositional conditions changed frequently, in accordance with the very dynamic nature of the backbarrier tidal flat area. The time span needed for the sedimentation of the studied layers may differ significantly. For instance, sediment redistribution may occur due to wave action during storms (Chang et al. 2006a, b; Christiansen et al. 2006).

DOC, sulphate, and metabolic products in pore waters

The depth trends of sulphate, DOC, nutrients, several metabolic products, chloride, and pH (Fig. 5) are typical for the sampling site and were chosen as representative example for the sampling period from May 2005 to June 2006. Concentrations change to some extent within the sampling period of 1 year, however the trends with depth remain the same.

Concentrations of Cl^- vary around 500 mM over the entire depth profile with a minimum concentration of 480 mM at 0.75 m depth. Consequently, no subterranean fresh water contribution from the nearby mainland influences the salinity at the sampling site. The pH values vary between 7.8 in the upper part of the sediment and 6.9 at 5 m depth.

Fig. 5 Pore water profiles of Cl^-, pH, NO_3^-, SO_4^{2-}, H_2S, CH_4, H_4SiO_4, TA, NH_4^+, PO_4^{3-}, and DOC at the sampling site in an intertidal sand flat of the backbarrier area of Spiekeroog Island (April 2006; CH_4 March 2006). DIC concentrations were calculated using TA and pH
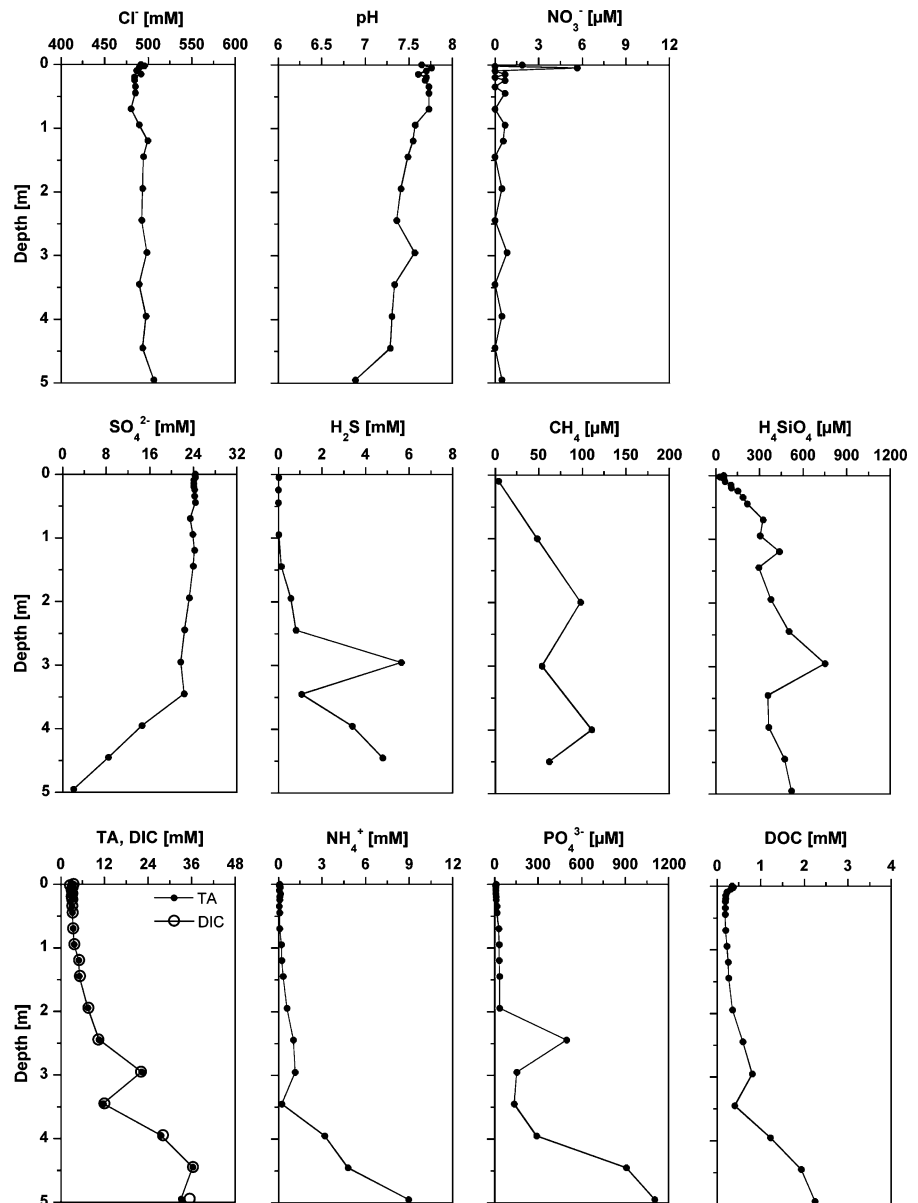
Nitrate pore water concentrations are below 1 μM except at 5 cm depth where a concentration of 5.6 μM is determined. In contrast, sea water of the study area shows higher NO_3^- concentrations ranging from about 80 μM at the beginning of April to about 5 μM in May and June 2006 (Grunwald et al. 2007). The slightly elevated NO_3^- pore water concentration at 5 cm depth is either due to sea water introduced into the sediment, bioirrigation and/or nitrification. The generally low NO_3^- pore water concentrations imply that sea water NO_3^- introduced into surface sediments is rapidly denitrified.

Sulphate concentrations are close to the sea water value of 26 mM (at salinity 31 in the Wadden Sea) in the upper part of the sediment, followed by a decrease in SO_4^{2-} concentration. At a sediment depth of 5 m very low concentrations of SO_4^{2-} remain. Sulphate reducers were successfully identified in the study area. Sulphate reduction rates are in the low nM cm^{-3} d^{-1} range and reach up to 1 μM cm^{-3} d^{-1} in surface sediments of the backbarrier area of Spiekeroog Island (Böttcher et al. 2000; Wilms et al. 2006a,b). In tidal flats with mixed sand and clay composition, sulphate reduction rates remain in the low nM cm^{-3} d^{-1} range

Fig. 6 Modelled (continuous line) and measured (points) pore water profiles. Same samples as in Fig. 3. To test for sensitivity of the pore water profiles to organic matter composition, simulations were conducted with Redfield ratios increased and decreased by 50% (dashed lines)
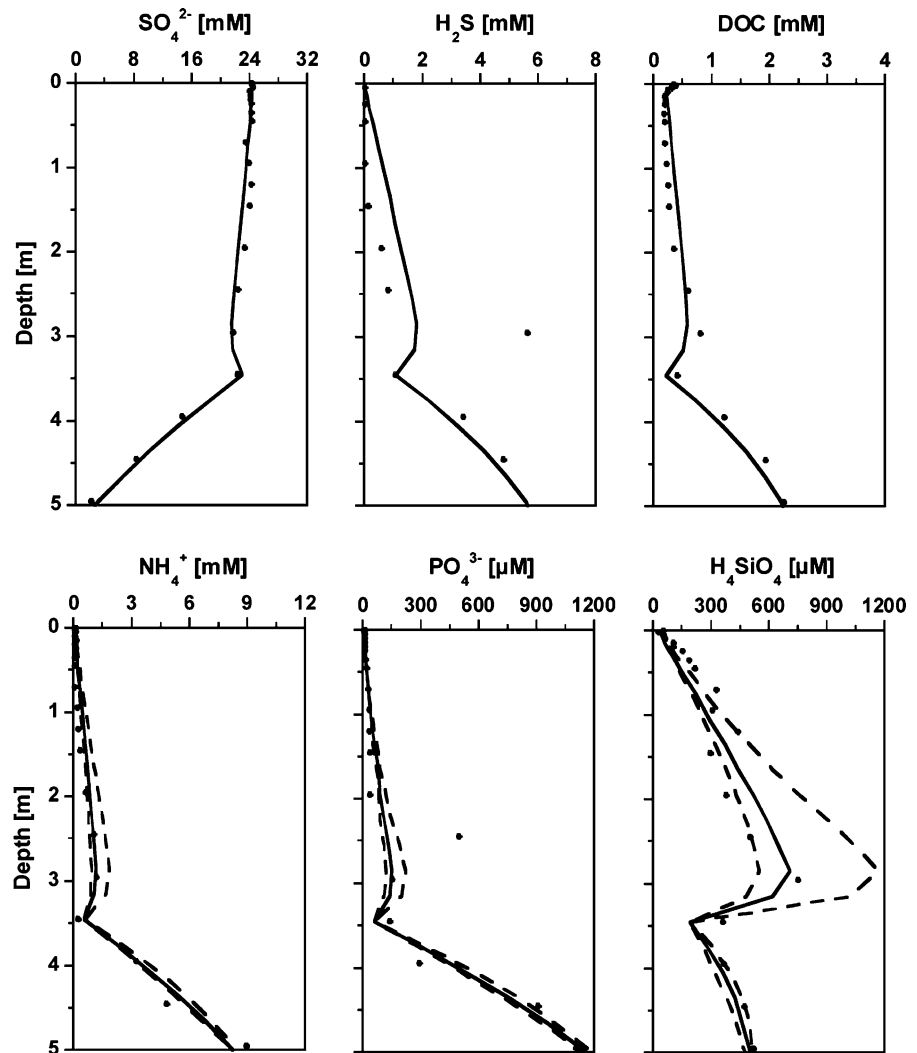
even in some metres depth (Wilms et al. 2006b). These values are comparable to sulphate reduction rates determined in other tidal flat systems (Kristensen et al. 2000; Gribsholt and Kristensen 2003).

Sulphide is the terminal metabolic product of sulphate reduction. In the sediment the concentration of sulphide is influenced by the formation of the iron sulphides FeS and FeS_2 (Howarth and Jørgensen 1984; Moeslund et al. 1994). In the study area, the formation of iron sulphides leads to low sulphide concentrations in the upper metres of the sediment. Modelled sulphide concentrations are higher than measured ones because the process of iron sulphide formation is not implemented in the model setup (Fig. 6). Modelling thus confirms the precipitation of iron sulphides. To a small extent sulphide oxidation

to sulphate may occur in these layers as well (Thamdrup et al. 1993). Sulphide concentrations do not constantly increase with decreasing sulphate concentrations. At 3 m depth, the sulphide concentration is high, although sulphate shows little depletion. This finding cannot be fully explained and is not reproduced in the model setup (Fig. 6). It may be due to entrapment of sulphide in or below a less permeable clay-rich sediment layer.

Methane shows concentrations of about 5 μM at the sediment surface, and increases to about 100 μM at greater depths. Methane concentrations already start to increase in a sediment depth of about 1 m, where high sulphate concentrations are still found. This illustrates the coexistence of sulphate reducers and methanogens (Wilms et al. 2006a), and most

notably, the upward diffusion of methane from its depth of production below 5 m depth towards the sediment surface.

At the sampling site, the sandy sediment surface is covered by ripples leading to advective pore water flow at the sediment surface (Huettel et al. 1996, Huettel and Rusch 2000). Thus, organic material is easily introduced into the upper layer of the sandy sediments and subsequently degraded aerobically and anaerobically. The degradation products are either used by microorganisms for their metabolism, take part in other biogeochemical reactions or become enriched in pore waters. The enrichment of DOC, NH_4^+, PO_4^{3-}, and TA with depth reflects the decomposition of organic matter. The increase in H_4SiO_4 concentrations mirrors the dissolution of biogenic silica. At shallower depths, where exchange between pore water and overlying water column occurs, these species show concentrations only slightly higher than in the sea water of the study area (Schnetger et al. 2001; Dellwig et al. 2007; Grunwald et al. 2007). In the model setup, exchange processes between sediment layers of some decimetres depth and the overlying water column are not considered. Therefore, measured concentrations are lower than modelled ones in the upper metre (Fig. 6).

Stoichiometry of organic matter degradation

$(SO_4^{2-})_{Dep}$ is positively correlated with TA, NH_4^+, PO_4^{3-}, and DOC. In Fig. 7A the correlations are displayed for samples taken in April 2006. To support these results, regression analyses were performed for all samples taken throughout 1 year from May 2005 until June 2006 (Fig. 7B). The ratio of TA:$(SO_4^{2-})_{Dep}$ is 1.7 for samples from April 2006 and changes only slightly if all samples analysed during a 1 year period are taken into account (Table 2). This ratio is close to the expected C:$(SO_4^{2-})_{Dep}$ ratio of 2, based on Redfield ratios and the assumption that organic matter is degraded by sulphate reduction. Methanogenesis is presumably responsible for organic matter degradation besides sulphate reduction at the study site, however to a much smaller extent. Estimates of the C:N ratio of degraded organic matter are 3.1 regarding samples of April 2006 and 2.8 for samples obtained during the whole sampling period of 1 year (Table 2). The C:P stoichiometry is 76 for samples

from April 2006 and 104 for all samples. The modelled C:N and C:P ratios are 3.5 and 77, respectively (Table 2).

Discussion

Terminal metabolic pathways

The oxidation of organic matter in sediments is coupled to electron acceptors, and thus depends on their reactivity and availability. Aerobic respiration is followed by nitrate reduction, reduction of Mn^{IV} and Fe^{III} oxides, sulphate reduction and finally methanogenesis (Froelich et al. 1979). Based on the availability of SO_4^{2-} compared to other electron acceptors, sulphate reduction dominates anaerobic carbon oxidation in marine subsurface sediments (Jørgensen 1982).

In this study, pore water profiles are used to evaluate the pathways of organic matter degradation in an intertidal flat, with focus on depths exceeding 1 m. At the study site bottom flow interacting with sediment ripples generates an intrusion of oxygenated water into the sediment surface. The surface layer where organic matter is remineralised aerobically thus extends to some centimetres depth (Billerbeck et al. 2006b). Nitrification, denitrification, and nitrate reduction seem to be closely coupled to each other in the surface sediment leading to low NO_3^- concentrations over the entire depth profile. Assuming that oxygen respiration and denitrification are restricted to sediment layers containing measurable oxygen and nitrate, these two processes are confined to the upper few centimetres of the sediment.

The tight coupling of products of organic matter degradation like NH_4^+, and PO_4^{3-} with $(SO_4^{2-})_{Dep}$ suggests that in anoxic sediment layers the organic matter is mainly degraded by sulphate reduction (Fig. 7). Sulphate concentrations remain at high levels down to 3.5 m depth and do attain concentrations close to zero only at 5 m depth. Sulphate reducing bacteria can metabolise labile organic matter when sulphate concentrations are exceeding ~ 1 mM (Alperin et al. 1994). Except at 5 m depth, enough sulphate is thus available as terminal electron acceptor for sulphate reducing bacteria. Pore water advection within the sediment may lead to an underestimation of the sulphate reduced in the

Fig. 7 Ratios of DOC, TA, NH_4^+, and PO_4^{3-} concentrations to $(SO_4^{2-})_{Dep}$ concentrations. Best-fit linear regressions are calculated for samples from April 2006 separately (**A**) and for all samples taken from May 2005 till June 2006 (**B**)
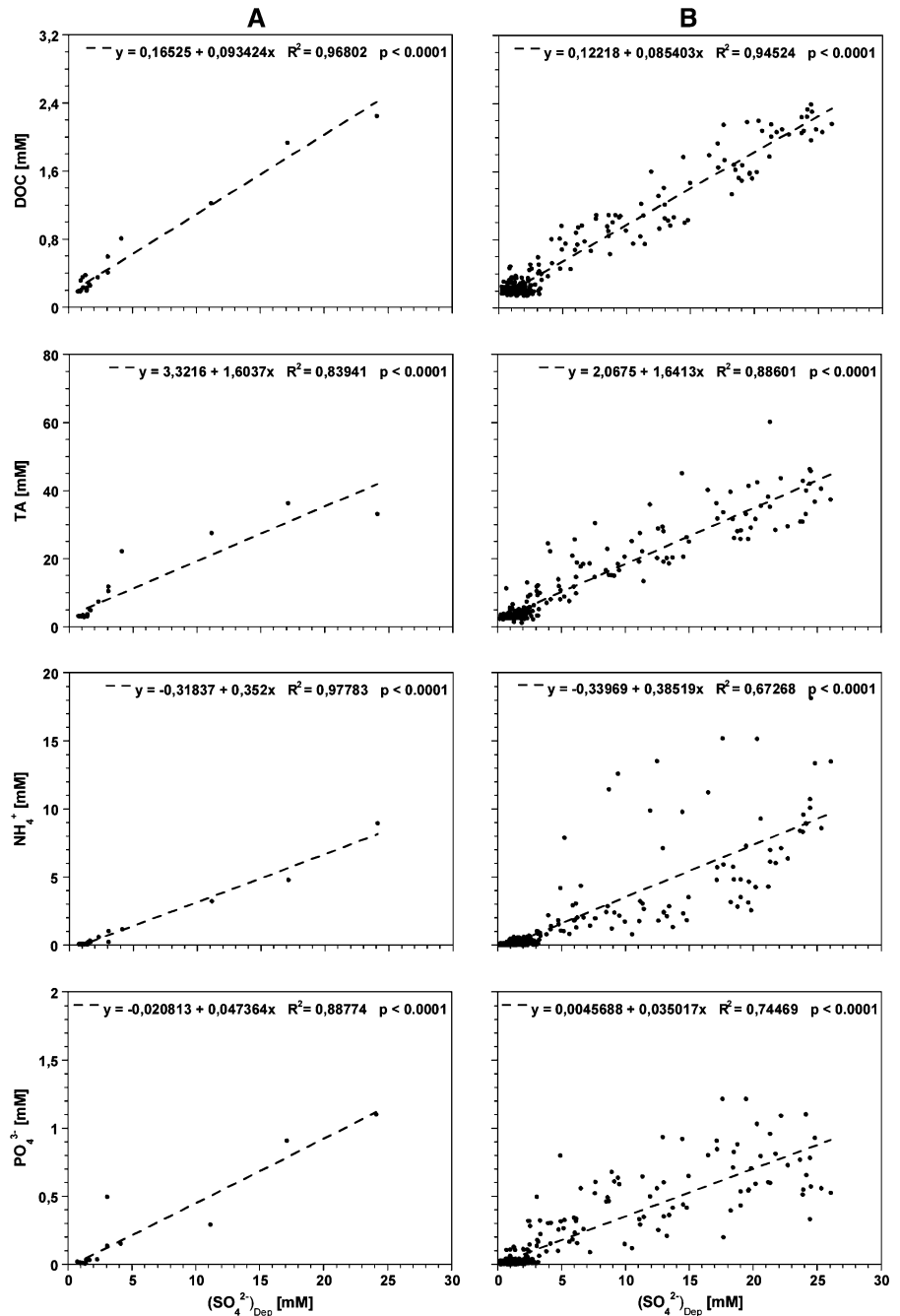
sediment. The relatively constant sulphate concentrations in the permeable sandy layers down to 2 m depth point towards a replenishment of sulphate by sea water and/or pore water from central parts of the tidal flat. Nevertheless, the general conclusion concerning the importance of sulphate reduction for anaerobic organic matter degradation remains valid. Weston et al. (2006) drew similar conclusions

regarding the relevance of organic matter remineralisation pathways for intertidal creek-bank sediments in Georgia and South Carolina, USA.

A conclusion about the depth of methane production can hardly be drawn. Due to concentration gradients and pressure fluctuations induced by tidal cycles, methane will supposedly migrate slowly from its depth of production towards the sediment surface.

Table 2 Stoichiometry during organic matter degradation estimated from slopes of pore water concentrations of total alkalinity TA and sulphate depletion $(SO_4^{2-})_{Dep}$ against NH_4^+ and PO_4^{3-} concentrations for samples of April 2006 and for samples taken from May 2005 to June 2006

	$C:SO_4^{2-}$	C:N	C:P
Suspended particulate matter		7.8[a]	
Sediment April 2005		8.6	
Pore water April 2006			
TA	1.7	3.2	77
$(SO_4^{2-})_{Dep}$		3.0	75
Pore water model April 2006		3.5	77
Pore water May 2005–June 2006			
TA	1.8	2.8	106
$(SO_4^{2-})_{Dep}$		2.7	101

The ratios of suspended particulate matter and the ratios derived from modelling pore water profiles are further displayed

[a] Lunau et al. (2006)

The main zone of production may be located below 5 m depth where sulphate is depleted. In spite of minor methanogenesis occurring in sediment layers down to 5 m depth, sulphate reduction dominates anaerobic organic matter remineralisation. This conclusion is supported by the model results. Depth profiles of sulphate, DOC, and nutrients are reproduced in the model setup where sulphate reduction was assumed to be the anaerobic remineralisation process (Fig. 6).

Organic matter remineralisation

DOC concentrations correlate very well with $(SO_4^{2-})_{Dep}$, with maxima in the zone of maximum sulphate depletion (Fig. 7). However, it is not evident if this correlation is reflecting a single biogeochemical process involving DOC and SO_4^{2-}. Hydrolysis and fermenting microorganisms could have converted organic matter leading to the production of refractory and labile DOC, whereas the labile part is used by sulphate reducers (Böttcher et al. 1997; Rusch et al. 1998).

The organic matter mineralised at the sampling site is richer in N and P than expected from the Redfield ratio (Table 2). The C:N and C:P ratios according to Redfield are 6.6 and 106, respectively. We assume that the regression technique yields valuable results, although certain sediment layers are influenced by advection. Advection mainly occurs

in sediment layers above 3 m depth and to a small extent at 3.5 m depth. Regression analyses are however dominated by pore water results from below 3 m depth where sulphate depletion of more than 4 mM is calculated and advection is of minor importance.

The deviation from the Redfield ratios does not represent a completely unexpected finding as the Redfield ratio is based on average oceanic relationships. In intertidal creek bank sediments of South Carolina and Georgia (USA), C:N ratios as low as 3.4 were determined (Weston et al. 2006). The results further suggest that organic matter components containing nitrogen are degraded with higher priority. This finding is in accordance with Weston et al. (2006) who found preferential hydrolysis of particulate organic nitrogen relative to particulate organic carbon when organic matter mineralisation rates are high. In our study area, suspended particulate matter determined in the open water column has an average C:N ratio of 7.8 (Lunau et al. 2006). This suspended matter is partly incorporated into the sediment and in the following degraded by microorganisms (Huettel et al. 1996; Huettel and Rusch 2000; Rusch and Huettel 2000). The C:N ratio of about 3 calculated based on metabolic products in pore water is thus lower than the ratio determined for suspended particulate matter in the open water column suggesting preferential degradation of nitrogen containing compounds in the sediment. The C:N ratio of 8.6 determined for the organic matter in the sediment supports this hypothesis. It reflects an enrichment of carbon in sedimentary organic matter compared to suspended particulate matter.

Anaerobic oxidation of methane may occur in the sediment to a certain degree (K. Bischof, pers. commun.). This process consumes sulphate (Hensen et al. 2003) which would have led to an overestimation of the respiratory sulphate reduction. However, reducing the calculated sulphate depletion would result in even lower C:N ratios. Furthermore, ratios estimated from sulphate depletion and total alkalinity are similar suggesting that anaerobic oxidation of methane is unimportant in the upper 5 m of the sediment.

Modelling our pore water profiles results in C:N and C:P ratios similar to those calculated by regression analysis (Table 2). In the model, the unexpectedly high PO_4^{3-} concentration at 2.5 m

depth is disregarded. The exclusion of this PO_4^{3-} concentration in the model setup seems to be of importance. Regression analysis $(SO_4^{2-})_{Dep}$ against PO_4^{3-} without the PO_4^{3-} concentration at 2.5 m depth does not result in a significantly different C:P ratio. The estimations of C:N and C:P ratios by regression analysis are thus supported by the model results. In simulations, Redfield ratios were increased and decreased by 50% to test the sensitivity of the depth profiles to Redfield composition (Fig. 6) Due to the relative proximity of the advective to the reactive layer, the pore water profiles of NH_4^+, PO_4^{3-} and H_4SiO_4 are somewhat insensitive to variable Redfield ratios. This limits its use for validating the applicability of the regression technique but the robustness of the resulting pore water profiles supports the hypothesis of the advective layer.

Pore water profiles

Pore water depth profiles are controlled by biogeochemical, sedimentological, and hydrological processes. In general, sulphate, DOC, nutrients, total alkalinity, methane, and sulphide show either an increase or decrease with depth depending on whether the species are consumed or produced during organic matter remineralisation (Fig. 5). Despite the dynamic sedimentological conditions in the study area, the general depth profiles determined in the relatively young intertidal flat sediments of some metres depth are comparable to those of deep marine surface sediments (Sholkovitz 1973; Canfield et al. 1993a,b; Thamdrup and Canfield 1996; Mäkelä and Tuominen 2003).

At the study site, concentration gradients do not always increase or decrease continuously with depth. At depths exceeding 3.5 m, sulphate shows a stronger depletion with depth than in the overlying sediment layers, whereas DOC, ammonium and phosphate exhibit a more pronounced enrichment. This is probably due to a displacement of the tidal flat margin. Within 14 years the eastern tidal flat margin of the Janssand was displaced about 100 m to the east (B.W. Flemming pers. comm.) suggesting that the sampling site may formerly have been located close to the low tide water line in contrast to its recent position 75 m afar from it. In the study area, tidal flat margins show a high microbial activity, especially near the low tide water line, resulting in high nutrient

concentrations (Billerbeck et al. 2006b). Sediments at depths exceeding 4 m which show enrichments in nutrients and DOC thus probably formed part of the former tidal flat margin.

In permeable sediments, pore water depth profiles may be further influenced by pore water advection. In several studies, advection processes were described in tidal flat sediments (Whiting and Childers 1989; Howes and Goehringer 1994; Billerbeck et al. 2006a, b; Wilson and Gardner 2006). All these studies were carried out close to tidal flat margins where at low tide a hydraulic gradient is generated between the pore water level in the tidal flat and the water level in the tidal creek. There is evidence that advection occurs in specific sediment depths at our sampling site. For example, NH_4^+ shows an unexpected low concentration at 3.5 m depth. The sediment is lithologically composed of layers with different porosities and permeabilities. At 3.5 m depth, a sediment layer which is more permeable than the layers above and below promote water flow. In the sediment core this permeable layer is geochemically identified as a sandy layer below 3 m depth owing to its high SiO_2 content. The depth of the permeable layer in the sediment core does not exactly match the depth of low NH_4^+ concentrations at the pore water sampling site due to slight compression of the sediment core during vibration coring. The NH_4^+ depth profile thus implies that NH_4^+ concentrations at 3.5 m depth are influenced by deep pore water advection. The NH_4^+ minimum at 3.5 m depth may be caused by channelled pore water flow from central parts of the sand flat where average NH_4^+ concentrations of about 0.4 mM are determined down to 3.5 m depth. DOC and total alkalinity further show lower concentrations at 3.5 m depth compared to intervals above and below. In the model setup, the shape of the pore water profiles is well reproduced when non-local transport is implemented in the model as surrogate process for advection at 3.5 m depth. The only exceptions are the sulphide concentration at 3 m depth and the PO_4^{3-} concentration at 2.5 m depth. The model results thus support the hypothesis that pore water exchange processes are influenced by advection besides diffusion.

At tidal flat margins, pore water flow generated by a hydraulic gradient may lead to the release of pore waters from creekbanks. This may have an impact on the chemistry of the overlying water column. In the

Fig. 8 Sea water PO_4^{3-} and H_4SiO_4 concentrations determined at a monitoring station in the backbarrier area of Spiekeroog Island in May 2006. The dashed line indicates the tidal variations of the sea water level
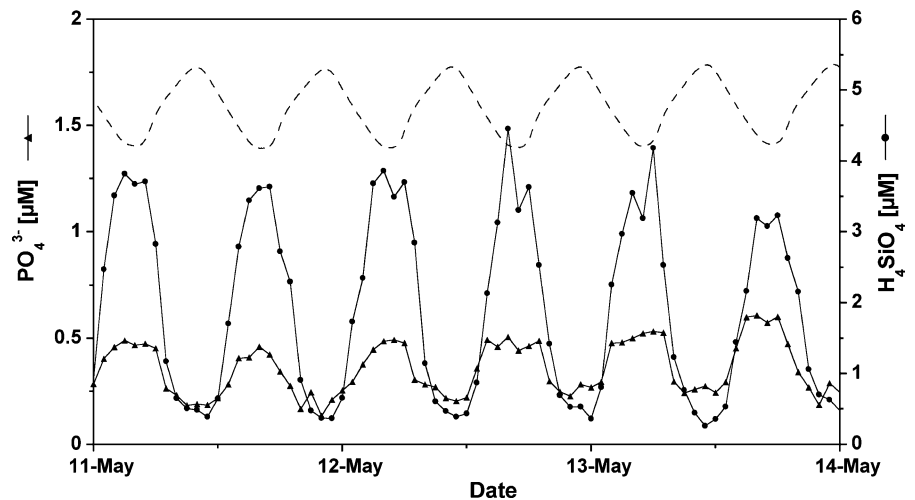
backbarrier area of Spiekeroog Island, PO_4^{3-} and H_4SiO_4 sea water concentrations vary depending on the state of the tidal cycle with higher concentrations being determined during low tide (Fig. 8). In the study area, concentrations in deep pore water are 10–1000 times higher than in sea water (Liebezeit et al. 1996; Schnetger et al. 2001; Grunwald et al. 2007). Pore water seepage at the tidal flat margin thus may explain increases in PO_4^{3-} and H_4SiO_4 concentrations in sea water during low tide. Our pore water concentrations determined several metres afar from the low tide water line do not completely equal those of seeping pore waters at the tidal flat margin. However, the results of our study give first insights into deep pore waters, which may be horizontally transported towards the tidal flat margin where they seep out of the sediment. Close to the low tide water line at the tidal flat margin, where most of the pore water seeps are found, the oxic layer of the sediment surface is very thin or even lacking. This suggests that the seeping pore waters may chemically only slightly be modified before entering the overlying water column.

Fresh water, which occasionally flows into the backbarrier area during low tide via a flood gate, may additionally represent a nutrient source. At the flood gate of Neuharlingersiel (Fig. 1) the average PO_4^{3-} and H_4SiO_4 concentrations determined in 2002 and 2003 were 4 μM and 110 μM, respectively (at salinities about 1). Fresh water concentrations are lower than deep pore water concentrations (Fig. 5) and fresh water does not flow into the backbarrier area during every low tide. Fresh water thus

presumably releases a smaller amount of nutrients into the backbarrier area compared to pore water.

Conclusions

For the first time, biogeochemical processes are described in tidal flat sediments of some metres depth. Despite the dynamic sedimentological conditions in the study area, the general depth profiles obtained in the relatively young intertidal flat sediments of some metres depth are comparable to those determined in deep marine surface sediments. Lithological and hydrological conditions however exert influence on sulphate, DOC, and nutrient pore water profiles. In some sediment layers advective flow occurs besides diffusive transport. Due to the hydraulic gradient generated at tidal flat margins during low tide between the pore water level and the water level in the tidal creek, pore waters rich in remineralisation products are transported towards the tidal flat margin. The release of these nutrient-rich pore waters at creekbanks may account for the increase in sea water nutrient concentrations in the study area during low tide.

Sulphate reduction has been identified as the most important pathway for anaerobic organic matter remineralisation. Pore water concentrations of sulphate, ammonium, and phosphate have been used to elucidate the composition of organic matter degraded in the sediment. The calculated C:N and C:P ratios are below the Redfield ratio. Preferential hydrolysis of particulate organic nitrogen relative to particulate

organic carbon may explain the low C:N ratios of about 3. Model results support the results concerning the composition of remineralised organic matter and the importance of sulphate reduction as the dominant anaerobic remineralisation process.

References

Alperin MJ, Albert DB, Martens CS (1994) Seasonal variations in production and consumption rates of dissolved organic carbon in an organic-rich coastal sediment. Geochim Cosmochim Acta 58:4909–4930. doi:10.1016/0016-7037(94)90221-6

Baldock JA, Masiello CA, Gélinas Y, Hedges JI (2004) Cycling an decomposition of organic matter in terrestrial and marine ecosystems. Mar Chem 92:39–64. doi:10.1016/j.marchem.2004.06.016

Beck M, Dellwig O, Kolditz K, Freund H, Liebezeit G, Schnetger B et al (2007) In situ pore water sampling in deep intertidal flat sediments. Limnol Oceanogr Methods 5:136–144

Beck M, Dellwig O, Liebezeit G, Schnetger B, Brumsack H-J (2008) Spatial and seasonal variations of sulphate, dissolved organic carbon, and nutrients in deep pore waters of intertidal flat sediment. Estuar Coast Shelf Sci. doi:10.1016/j.ecss.2008.04.007

Billerbeck M, Werner U, Bosselmann K, Walpersdorf E, Huettel M (2006a) Nutrient release from an exposed intertidal sand flat. Mar Ecol Prog Ser 316:35–51. doi:10.3354/meps316035

Billerbeck M, Werner U, Polerecky L, Walpersdorf E, de Beer D, Huettel M (2006b) Surficial and deep pore water circulation governs spatial and temporal scales of nutrient recycling in intertidal sand flat sediment. Mar Ecol Prog Ser 326:61–76. doi:10.3354/meps326061

Böttcher ME, Rusch A, Höpner T, Brumsack H-J (1997) Stable sulfur isotope effects related to local intense sulfate reduction in a tidal sandflat (Southern North Sea): results from loading experiments. Isotopes Environ Health Stud 33:109–129. doi:10.1080/10256019708036345

Böttcher ME, Oelschläger B, Höpner T, Brumsack H-J, Rullkötter J (1998) Sulfate reduction related to the early diagenetic degradation of organic matter and 'black spot' formation in tidal sandfalts of the German Wadden Sea (southern North Sea): stable isotope (^{13}C, ^{34}S, ^{18}O) and other geochemical results. Org Geochem 29:1517–1530. doi:10.1016/S0146-6380(98)00124-7

Böttcher ME, Hespenheide B, Llobet-Brossa E, Beardsley C, Larsen O, Schramm A et al (2000) The biogeochemistry, stable isotope geochemistry, and microbial community structure of a temperate intertidal mudflat: an integrated study. Cont Shelf Res 20:1749–1769. doi:10.1016/S0278-4343(00)00046-7

Boudreau BP (1992) A kinetic model for microbic organic-matter decomposition in marine sediments. FEMS Microbiol Ecol 102:1–14. doi:10.1111/j.1574-6968.1992.tb05789.x

Boudreau BP (1997) Diagenetic models and their implications. Springer, Berlin

Caetano M, Falcão M, Bebianno MJ (1997) Tidal flushing of ammonium, iron and manganese from inter-tidal sediment pore waters. Mar Chem 58:203–211. doi:10.1016/S0304-4203(97)00035-2

Canfield DE, Jørgensen BB, Fossing H, Glud R, Gundersen J, Ramsing NB et al (1993a) Pathways of organic carbon oxidation in three continental margin sediments. Mar Geol 113:27–40. doi:10.1016/0025-3227(93)90147-N

Canfield DE, Thamdrup B, Hansen JW (1993b) The anaerobic degradation of organic matter in Danish coastal sediments: Iron reduction, manganese reduction, and sulphate reduction. Geochim Cosmochim Acta 57:3867–3883. doi:10.1016/0016-7037(93)90340-3

Chang TS, Flemming BW, Tilch E, Bartholomä A, Wöstmann R (2006a) Late Holocene stratigraphic evolution of a back-barrier tidal basin in the East Frisian Wadden Sea, southern North Sea: transgressive deposition and its preservation potential. Facies 52:329–340. doi:10.1007/s10347-006-0080-2

Chang TS, Bartholomä A, Flemming BW (2006b) Seasonal dynamics of fine-grained sediments in a back-barrier tidal basin of the German Wadden Sea (Southern North Sea). J Coast Res 22:328–338. doi:10.2112/03-0085.1

Charette MA, Sholkovitz ER (2006) Trace element cycling in a subterranean estuary: Part 2 Geochemistry of the pore water. Geochim Cosmochim Acta 70:811–826. doi:10.1016/j.gca.2005.10.019

Christiansen C, Vølund G, Lund-Hansen LC, Bartholdy J (2006) Wind influence on tidal flat sediment dynamics: field investigations in the Ho Bugt, Danish Wadden Sea. Mar Geol 235:75–86. doi:10.1016/j.margeo.2006.10.006

De Beer D, Wenzhöfer F, Ferdelman TG, Boehme SE, Huettel M, van Beusekom JEE et al (2005) Transport and mineralization rates in North Sea sandy intertidal sediments, Sylt-Rømø Basin, Wadden Sea. Limnol Oceanogr 50:113–127

Delafontaine MT, Bartholomä A, Flemming BW, Kurmis R (1996) Volume-specific dry POC mass in surficial intertidal sediments: a comparison between biogenic muds and adjacent sand flats. Senckenb Marit 26:167–178

Dellwig O, Hinrichs J, Hild A, Brumsack H-J (2000) Changing sedimentation in tidal flat sediments of the southern North Sea from the Holocene to the present: a geochemical

approach. J Sea Res 44:195–208. doi:10.1016/S1385-1101(00)00051-4

Dellwig O, Bosselmann K, Kölsch S, Hentscher M, Hinrichs J, Böttcher ME et al (2007) Sources and fate of manganese in a tidal basin of the German Wadden Sea. J Sea Res 57:1–18. doi:10.1016/j.seares.2006.07.006

Flemming BW, Davis RA Jr (1994) Holocene evolution, morphodynamics and sedimentology of the Spiekeroog barrier island system (Southern North Sea). Senckenb Marit 24:117–155

Froelich PN, Klinkhammer GP, Bender ML, Luedtke NA, Heath GR, Cullen D et al (1979) Early oxidation of organic matter in pelagic sediments of the eastern equatorial Atlantic: suboxic diagenesis. Geochim Cosmochim Acta 43:1075–1090. doi:10.1016/0016-7037(79)90095-4

Grasshoff K, Kremling K, Ehrhardt M (1999) Methods of seawater analysis. Wiley-VCH, New York

Gribsholt B, Kristensen E (2003) Benthic metabolism and sulfur cycling along an inundation gradient in a tidal spartina anglica salt marsh. Limnol Oceanogr 48:2151–2162

Grunwald M, Dellwig O, Liebezeit G, Schnetger B, Reuter R, Brumsack H-J (2007) A novel time-series station in the Wadden Sea (NW Germany): first results on continuous nutrient and methane measurements. Mar Chem 107:411–421. doi:10.1016/j.marchem.2007.04.003

Hensen C, Zabel M, Pfeifer K, Schwenk T, Kasten S, Riedinger N et al (2003) Control of sulfate pore-water profiles by sedimentary events and the significance of anaerobic oxidation of methane for the burial of sulfur in marine sediments. Geochim Cosmochim Acta 67:2631–2647. doi:10.1016/S0016-7037(03)00199-6

Howarth RW, Jørgensen BB (1984) Formation of ^{35}S-labelled elemental sulfur and pyrite in coastal marine sediments (Limfjorden and Kysing Fjord, Denmark) during short-term $^{35}SO_4^{2-}$ reduction measurements. Geochim Cosmochim Acta 48:1807–1818. doi:10.1016/0016-7037(84)90034-6

Howes BL, Goehringer DD (1994) Porewater drainage and dissolved organic carbon and nutrient losses through the intertidal creekbanks of a New England salt marsh. Mar Ecol Prog Ser 114:289–301. doi:10.3354/meps114289

Huettel M, Rusch A (2000) Transport and degradation of phytoplankton in permeable sediment. Limnol Oceanogr 45:534–549

Huettel M, Ziebis W, Forster S (1996) Flow-induced uptake of particulate matter in permeable sediments. Limnol Oceanogr 41:309–322

Huettel M, Ziebis W, Forster S, Luther GWIII (1998) Advective transport affecting metal and nutrient distributions and interfacial fluxes in permeable sediments. Geochim Cosmochim Acta 62:613–631. doi:10.1016/S0016-7037(97)00371-2

Jahnke RA, Alexander CR, Kostka JE (2003) Advective pore water input of nutrients to the Satilla river estuary, Georgia, USA. Estuar Coast Shelf Sci 56:641–653. doi:10.1016/S0272-7714(02)00216-0

Jørgensen BB (1982) Mineralization of organic matter in the sea bed–the role of sulphate reduction. Nature 296:643–645. doi:10.1038/296643a0

Kristensen E, Bodenbender J, Jensen MH, Rennenberg H, Jensen KM (2000) Sulfur cycling of intertidal Wadden Sea sediments (Königshafen, Island of Sylt, Germany): sulfate reduction and sulfur gas emission. J Sea Res 43:93–104. doi:10.1016/S1385-1101(00)00007-1

Kuwae T, Kibe E, Nakamura Y (2003) Effect of emersion and immersion on the porewater nutrient dynamics of an intertidal sandflat in Tokyo Bay. Estuar Coast Shelf Sci 57:929–940. doi:10.1016/S0272-7714(02)00423-7

Lewis E, Wallace DWR (1998) Program developed for CO_2 system calculations. ORNL/CDIAC-105. Carbon Dioxide Information Analysis Center, Oak Ridge National Laboratory U.S. Department of Energy, Oak Ridge

Liebezeit G, Behrends B, Kraul T (1996) Variability of nutrients and particulate matter in backbarrier tidal flats of the East Frisian Wadden Sea. Senckenbergiana 26:195–202

Lunau M, Lemke A, Dellwig O, Simon M (2006) Physical and biogeochemical controls of microaggregate dynamics in a tidally affected coastal ecosystem. Limnol Oceanogr 51:847–859

Magni P, Montani S (2006) Seasonal patterns of pore-water nutrients, benthic chlorophyll a and sedimentary AVS in a macrobenthos-rich tidal flat. Hydrobiologia 571:297–311. doi:10.1007/s10750-006-0242-9

Mäkelä K, Tuominen L (2003) Pore water nutrient profiles and dynamics in soft bottoms of the northern Baltic Sea. Hydrobiologia 492:43–53. doi:10.1023/A:1024809710854

Mayer LM (1994) Relationships between mineral surfaces and organic carbon concentrations in soils and sediments. Chem Geol 114:347–363. doi:10.1016/0009-2541(94)90063-9

Moeslund L, Thamdrup B, Jørgensen BB (1994) Sulfur and iron cycling in a coastal sediment: radiotracer studies and seasonal dynamics. Biogeochemistry 27:129–152

Murray LG, Mudge SM, Newton A, Icely JD (2006) The effect of benthic sediments on dissolved nutrient concentrations and fluxes. Biogeochemistry 81:159–178. doi:10.1007/s10533-006-9034-6

Precht E, Huettel M (2004) Rapid wave-driven advective pore water exchange in a permeable coastal sediment. J Sea Res 51:93–107. doi:10.1016/j.seares.2003.07.003

Precht E, Franke U, Polerecky L, Huettel M (2004) Oxygen dynamics in permeable sediments with wave driven pore water exchange. Limnol Oceanogr 49:693–705

Rusch A, Huettel M (2000) Advective particle transport into permeable sediments-evidence form experiments in an intertidal sandflat. Limnol Oceanogr 45:525–533

Rusch A, Töpken H, Böttcher ME, Höpner T (1998) Recovery from black spots: results of a loading experiment in the Wadden Sea. J Sea Res 40:205–219. doi:10.1016/S1385-1101(98)00030-6

Rusch A, Forster S, Huettel M (2001) Bacteria, diatoms and detritus in an intertidal sandflat subject to advective transport across the water-sediment interface. Biogeochemistry 55:1–27. doi:10.1023/A:1010687322291

Rusch A, Huettel M, Wild C, Reimers CE (2006) Benthic oxygen consumption and organic matter turnover in organic-poor, permeable shelf sands. Aquat Geochem 12:1–19. doi:10.1007/s10498-005-0784-x

Sarazin G, Michard G, Prevot F (1999) A rapid and accurate spectroscopic method for alkalinity measurements in sea

water samples. Water Res 33:290–294. doi:10.1016/S0043-1354(98)00168-7

Schnetger B, Hinrichs J, Dellwig O, Shaw T, Brumsack H-J (2001) The significance of radionuclides and trace elements in a back barrier tidal area: results from the German Wadden Sea. In: Inaba J, Hisamatsu S, Ohtsuka Y (eds) Proceedings of the international workshop on distribution and speciation of radionuclides in the environment, Rokkasho, Aomori, Japan, October 2000, pp 99–106

Sholkovitz E (1973) Interstitial water chemistry of the Santa Barbara Basin sediments. Geochim Cosmochim Acta 37:2043–2073. doi:10.1016/0016-7037(73)90008-2

Sørensen J, Jørgensen BB, Revsbech NP (1979) A comparison of oxygen, nitrate, and sulfate respiration in coastal marine sediments. Microb Ecol 5:105–115. doi:10.1007/BF02010501

Thamdrup B, Canfield DE (1996) Pathways of carbon oxidation in continental margin sediments off central Chile. Limnol Oceanogr 41:1629–1650

Thamdrup B, Finster K, Würgler Hansen J, Bak F (1993) Bacterial disproportionation of elemental sulfur coupled to chemical reduction of iron or manganese. Appl Environ Microbiol 59:101–108

Wedepohl KH (1971) Environmental influence on the chemical composition of shales and clays. In: Ahrens LH, Press F, Runcorn SK, Urey HC (eds) Physics and chemistry of the earth, vol 8. Pergamon, Oxford, pp 305–333

Weston NB, Porubsky WP, Samarkin VA, Erickson M, Macavoy SE, Joye SB (2006) Porewater stoichiometry of terminal metabolic products, sulfate, and dissolved organic carbon and nitrogen in estuarine intertidal creek-bank sediments. Biogeochemistry 77:375–408. doi:10.1007/s10533-005-1640-1

Whiting GJ, Childers DL (1989) Subtidal advective water flux as a potentially important nutrient input to Southeastern U.S.A. saltmarsh estuaries. Estuar Coast Shelf Sci 28:417–431. doi:10.1016/0272-7714(89)90089-9

Wilms R, Sass H, Köpke B, Cypionka H, Engelen B (2006a) Methane and sulfate profiles within the subsurface of a tidal flat are reflected by the distribution of sulfate-reducing bacteria and methanogenic archaea. FEMS Microbiol Ecol. doi:10.1111/j.1574–6941.2006.00225.x

Wilms R, Köpke B, Sass H, Chang TS, Cypionka H, Engelen B (2006b) Deep biosphere-related bacteria within the subsurface of tidal flat sediments. Environ Microbiol 8:709–719. doi:10.1111/j.1462-2920.2005.00949.x

Wilson AM, Gardner LR (2006) Tidally driven groundwater flow and solute exchange in a marsh: numerical simulations. Water Resour Res 42:W01405. doi:10.1029/2005WR004302

Wirtz K (2003) Control of biochemical cycling by mobility and metabolic strategies of microbes in the sediments: an integrated model study. FEMS Microbiol Ecol 46:295–306. doi:10.1016/S0168-6496(03)00196-X

Ziebis W, Huettel M, Forster S (1996) Impact of biogenic sediment topography on oxygen fluxes in permeable seabeds. Mar Ecol Prog Ser 140:227–237. doi:10.3354/meps140227